

# Determination of the scattering length for Rb-Cs $X^1\Sigma^+$ ground electronic state using a variational method

M. N. Guimarães<sup>‡</sup> and F. V. Prudente<sup>§</sup>

Instituto de Física, Universidade Federal da Bahia, 40170-115, Salvador, Bahia, Brazil.

## Abstract.

We performed the calculation of the scattering length for the elastic collision between the rubidium and cesium atoms. For this we applied a variational procedure based on the  $R$ -matrix theory for unbound states employing the finite element method (FEM) for expansion of the wave-function in terms of a finite set of local basis functions. The FEM presents as advantages the possibility of the development of a efficient matrix inversion algorithm which significantly reduces the computation time to calculate the  $R$  matrix. We also tested a potential energy curve with spectroscopic accuracy obtained before from a direct adjustment procedure of experimental data of the  $X^1\Sigma^+$  state based on genetic algorithm. The quality of our result was evaluated by comparing them with several ones previously published at literature.

PACS numbers: 30.50.Cx; 02.70.Dh; 03.65.Nk; 31.50.Bc

Submitted to: *arXiv*

## 1. Introduction

Especially in recent years, researches on ultracold atoms have led to important discoveries in atomic physics, notably the observation of Bose-Einstein condensation in gases of alkali atoms [1]. The collision with a second atom has been attracting interest because, among other things, opens the possibility of systematically cooling one of the atomic species. From the theoretical viewpoint, ultracold collisions involve very large interatomic distances, typically in the order of thousands of bohr, which makes difficult the numerical solution of the scattering problem. In the study of elastic collision between two atoms we consider the knowledge of the potential energy curve for short and long internuclear distances, and the asymptotic physical quantities are expressed in terms of  $S$ -matrix and phase shift obtained using the partial waves decomposition. In

<sup>‡</sup> mng@ufba.br

<sup>§</sup> prudente@ufba.br

particular, the scattering length, in sign and magnitude, enables to know the character of the interaction between atoms at very low energies.

Among the motivations for studying the cold and ultracold collision between the rubidium and cesium atoms is that the RbCs molecule has been subject of several recent spectroscopy studies [2–9]. In fact, it is the heaviest heteronuclear alkali diatomic molecule with the largest permanent dipole moment being a candidate for experiments with dense ultracold ensembles. The Bose-Einstein condensate has been successfully obtained for both atomic species, and cold, and ultracold, molecules, specially for the  $X^1\Sigma^+$  ground electronic state, have been produced, as well as, collisional properties have been calculated. Studies of ultracold atomic mixtures could also be important in applications in quantum computing.

In the theoretical studies of cold and ultracold collisions the variational methods have been unusual because of large matrices produced due to the very long range of potential. However, these procedures have proven to be a very powerful tool in developing numerical solutions for problems involving quantum scattering processes [10]. There are a broad range of approaches leading to many different problems. In all of them the solution is expanded in terms of known basis functions and the coefficients of expansion are determined by solving a set of linear algebraic equations, yielding at last the scattering observables. In particular, a procedure that has contributed to the recent progress is the  $R$ -matrix method originally proposed in 1947 by Wigner and Eisenbud [11] in the nuclear physics context, but which has been applied to several problems in atomic and molecular physics [12]. The variational principle via the  $R$ -matrix theory is formulated so as to lead to a problem of matrix inversion yielding as a result the  $R$  matrix, which is then connected to the  $S$  matrix.

The success of the variational calculation will depend on the correct choice of basis set; if it is appropriate to the problem, then the results will be accurate and it will be required a lower computational effort for execution of problem solution. For this purpose, a very accurate procedure is the finite element method (FEM). The FEM has been widely used in the analysis of engineering problems, but over the years it has been applied in both study of bound states as for scattering processes of quantum systems [13–18]. As a variational approach, in addition to provides a means to systematically improve the accuracy in the calculations in a natural way, the FEM has as advantages the possibility of the development of a efficient matrix inversion algorithm which significantly reduces the computation time to calculate the  $R$  matrix.

In this paper we performed the calculation of the scattering length for the elastic collision between the Rb and Cs pairs using the variational  $R$ -matrix and finite element methods which are presented in section 2. We also tested a potential energy curve with spectroscopic accuracy obtained before from a direct adjustment procedure of experimental data of the  $X^1\Sigma^+$  state based on genetic algorithm. The results are presents in section 3.

## 2. Methodology

### 2.1. Variational $R$ -matrix method

According to the variational formalism, the problem of solving the radial Schrödinger equation for a system composed by two atoms is equivalent to finding the solutions of the following functional of energy

$$J_l[\chi_l] = \int dr \chi_l^*(r) \left\{ -\frac{\hbar^2}{2\mu} \frac{d^2}{dr^2} + V_l^{ef}(r) - E \right\} \chi_l(r), \quad (1)$$

where  $l$  designates quantum number associated with the angular momentum,  $\mu$  is the reduced mass,  $\chi_l(r)$  is the radial solution and  $V_l^{ef}(r) = V(r) + \frac{\hbar^2 l(l+1)}{2\mu r^2}$  is the effective potential, where  $V(r)$  the potential energy curve.

The  $R$ -matrix method relates the wave function with its normal derivative on the boundary surface between the asymptotic and interaction regions defined by the point  $r = r_{max}$ . In particular, this method in variational form specifies that

$$\chi_l(r_{max}) = R_l \left. \frac{d\chi_l(r)}{dr} \right|_{r_{max}}, \quad (2)$$

where  $R_l$  is the  $R$  matrix for given  $l$ .

In order to have  $R_l$ , we expand the radial wave function in a finite set of basis functions,

$$\chi_l(r) = \sum_{j=1}^p c_j^l f_j(r), \quad (3)$$

replace this expansion, and the condition (2), in the functional (1) and impose the stationarity condition obtaining the  $R$  matrix for a collision process with one asymptotic channel:

$$R_l = \frac{\hbar^2}{2\mu} \sum_{i=1}^p \sum_{j=1}^p f_i^*(r_{max}) \{ \mathbf{B}_l^{-1} \}_{ij} f_j^*(r_{max}), \quad (4)$$

with  $\mathbf{B}_l \equiv \mathbf{H}_l - E\mathbf{O}$  where  $\mathbf{H}_l$  and  $\mathbf{O}$  are the Hamiltonian and Overlap matrices, respectively.

The relation between  $R_l$  and the scattering matrix for the  $l$ -th partial wave,  $S_l$ , can be achieved using the continuity of the function at point  $r = r_{max}$  and written in the form

$$S_l = e^{2i\delta_l} = \frac{[1 + ikR_l]}{[1 - ikR_l]} e^{-2i(kr_{max} - \frac{l\pi}{2})}, \quad (5)$$

where  $\delta_l$  is the phase shift and  $k = \sqrt{2\mu E/\hbar^2}$ . The scattering length,  $a$ , is related to the cross section for very small energies ( $k^2 \rightarrow 0$ ) wherein only waves with  $l = 0$  contribute to scattering and it is given by

$$-\frac{1}{a} = \lim_{k \rightarrow 0} [k \cot \delta_0]. \quad (6)$$

On the other hand, for small value of wave number,  $k$ , the phase shift, for  $l = 0$ , can be connected with the scattering length by the effective range expansion:

$$k \cot \delta_0 = -\frac{1}{a} + \frac{1}{2}r_c k^2 + O(k^4), \quad (7)$$

where  $r_c$  is the effective range [19–21]. Therefore, the scattering length, as well as the effective range, can also be calculated by equation (7).

A feature of the  $R$  variational formalism for scattering process is that, despite the  $S$  matrix be complex, the  $R$  matrix is real and ensures its symmetry and unitarity. On the other hand, a large computational effort is required the inversion of the matrix  $\mathbf{H}_l - E\mathbf{O}$  in order to obtaining  $R_l$  and such effort increases with the cube of the matrix order. But, this can be overcome by the finite element method which has great advantages when used to expand the function (3) and solve the equation (4).

## 2.2. Finite element method

The finite element method (FEM) applied to the current problem consists basically in divide the integration interval  $[0, r_{max}]$  into  $N_e$  elements, being the  $i$ th element defined in the range of  $r_{i-1}$  to  $r_i$  with  $r_0 = 0$  and  $r_{N_e} = r_{max}$ , and expand the radial wave function as follows

$$\chi(r) = \sum_{i=1}^{N_e} \sum_{j=0}^{n_i} c_j^i f_j^i(r), \quad (8)$$

where the parameter  $n_i$  is the highest order of the basis functions associated with the  $i$ th element,  $f_j^i(r)$  is the  $j$ th basis function of the same element and  $c_j^i$  are the expansion coefficients. Here, the  $l$ -index associated with the angular momentum has been omitted.

The functions  $\{f_j^i(r)\}$  satisfy the following property

$$f_j^i(r) = 0 \quad \text{if } r \notin [r_{i-1}, r_i]. \quad (9)$$

In particular, we utilizes, into each element, two interpolant functions,  $I_1^i \equiv f_0^i(r)$  and  $I_2^i \equiv f_{n_i}^i(r)$ , and polynomial shape functions,  $\mathcal{P}_j^i \equiv f_j^i(r)$  with  $j = 1, \dots, n_i - 1$  (see Ref. [22] for details). These basis functions have an important feature of that only the basis function  $I_2^{N_e} \equiv f_{n_{N_e}}^{N_e}(r)$  is non-null on the last node of the mesh:

$$f_j^i(r_{N_e}) = \begin{cases} 1 & \text{for } i = N_e, j = n_{N_e} \\ 0 & \text{otherwise} \end{cases}. \quad (10)$$

Because of equation (9), the elements of matricial representation of  $\widehat{B}$  operator have the following property:

$$\{\mathbf{B}\}_{jj'}^{ii'} = \int_a^b dr f_j^i(r) \widehat{B} f_{j'}^{i'}(r) = 0 \quad , \quad \forall i \neq i'. \quad (11)$$

This leads to matrices with an interesting block tridiagonal structure. Due to properties (11) and (10), when we utilize the FEM for expanding the radial wave functions (3) the  $R$  matrix (4) is written in the following form

$$R_l = \frac{\hbar^2}{2\mu} \{\mathbf{B}_l^{-1}\}^{N_e+1, N_e+1}, \quad (12)$$

where  $\mathbf{B}_l \equiv \mathbf{H}_l - E\mathbf{O}$  and the superscript indices in  $\mathbf{B}_l^{-1}$  represent its last block.

Therefore, we need to know only the last block of the inverse of  $\mathbf{H}_l - E\mathbf{O}$  matrix to obtain  $R_l$ . This can be done efficiently utilizing an algorithm developed by Prudente and Soares Neto [23] aiming to calculate only the last block of inverse matrix. It reduces significantly both the computational time to invert the matrix as the memory required to store it on the computer and is demonstrated in details in reference [24].

### 3. Results

In this section, data are presented to the elastic scattering of the cesium ( $^{133}\text{Cs}$ ) by rubidium ( $^{85}\text{Rb}$  and  $^{87}\text{Rb}$ ) atoms at temperatures close to absolute zero, interacting via the ground state ( $X^1\Sigma^+$ ) of the RbCs molecule. Specifically, we have presented scattering length and effective range calculations for the potential energy curve (PEC) obtained by Almeida *et al* [25] with spectroscopic accuracy from a direct adjustment procedure of experimental data based on the genetic algorithm. All calculations were performed using a computational implementation in Fortran based on variational  $R$ -matrix method and the finite element method (FEM). Shortly, for a partial wave with  $l = 0$ , we solve the matrix inversion problem, given by the equation (4) or (12), using the matrix inversion technique [24]. Having computed the  $R$  matrix, we then calculate the phase shift,  $\delta_0$ , from the equation (5). The scattering length,  $a$ , is obtained by its definition given by equation (6). The FEM uses the same polynomials order for all mesh elements (*i.e.*,  $n_i = \text{const.}, \forall i$ ) and the dimension of the  $\mathbf{B}_l = \mathbf{H}_l - E\mathbf{O}$  matrix is  $(N_e \cdot n_i + 1) \times (N_e \cdot n_i + 1)$  with its last block having dimension 1.

The analytic function used to represent the  $X^1\Sigma^+$  electronic state PEC of RbCs molecule is as follows

$$V(r) = \left( \sum_{i=1}^5 a_i r^{i-2} \right) e^{-(a_6 r + a_7 r^2)} - \sum_{k=3}^5 f_{2k}(a_8 r) \frac{C_{2k}}{r^{2k}}, \quad (13)$$

where

$$f_{2k}(a_8 r) = 1 - e^{-a_8 r} \sum_{i=0}^{2k} (a_8 r)^i / i!$$

are the Tang-Toennies damping functions [26]. This potential function was originally proposed by Korona *et al* [27], and its extension was performed by Patkowski *et al* [28] to describe the *ab initio* potential for argon dimer. Furthermore, Prudente *et al* [29] employed this potential function to adjusting *ab initio* PECs for the diatomic molecules LiH and H<sub>2</sub>. The numerical values of the  $\{a_j\}, j = 1, \dots, 8$  parameters and the

dispersion coefficients,  $C_n, n = 6, 8, 10$ , obtained by Almeida *et al* [25] are given in Table 1. In such paper they extended their previous methodology based on genetic algorithms [30] to fit the RbCs potential curve to spectroscopic data.

We also consider the potential proposed by Jamieson *et al* [31] who used their *ab initio* calculated short-range data matched at 17.9524 bohr to the analytical expression for long-range

$$V(r) = -\frac{C_6}{r^6} - \frac{C_8}{r^8} - \frac{C_{10}}{r^{10}} - Ar^\beta e^{-\gamma r} \quad (14)$$

with the parameters given in Table 2. In order to make a smooth connection between the two parts of the potential, it was joined the value of the long range potential, at 17.9524 bohr, the points *ab initio* calculated utilizing an interpolation scheme of short-range potential by cubic spline [32]. In the Figure 1 the PECs from equations (13) and (14) are represented with the parameters given in Tables 1 and 2, respectively.

Jamieson *et al* [31] used the Numerov's method to solve the radial Schrödinger equation for small asymptotic values of the wave number,  $k$ , determining the scattering length and effective range from the expansion (7). Employing the potential proposed by them, shown in Figure 1, they obtained the value of  $a = 40.24$  bohr, for the  $^{85}\text{Rb}-^{133}\text{Cs}$  collision, and,  $a = 60.18$  bohr, for the  $^{87}\text{Rb}-^{133}\text{Cs}$  collision. In turn, Zanelatto *et al* [33] also used the Numerov's method to determine the scattering length. Employing the same potential, they obtained the value of  $a = 40.357$  bohr, for the  $^{85}\text{Rb}-^{133}\text{Cs}$  collision, and,  $a = 60.610$  bohr, for the  $^{87}\text{Rb}-^{133}\text{Cs}$  collision.

To achieving a good accuracy of our results, we have divided the FEM integration region in two intervals, one associated with the interaction region and another with the asymptotic region, and we have used an equidistant mesh in each intervals with  $N_e = N_e^{in} + N_e^{out}$ . The scattering length as a function of the base parameters ( $N_e$  and  $n_i$ ) given in equation (8) is represented by  $a(N_e, n_i)$ . Specifically, to ensure a convergence factor,  $\Delta a = |a(N_e, n_i) - a(N_e, n_i - 1)|$ , of at least five decimal places, we have used  $N_e^{in} = 60$  in the interval of  $[0, 40]$  bohr,  $N_e^{out} = 50$  in the interval of  $[40, r_{max}]$  bohr and  $n_i = 30, \forall i$ . This convergence process is demonstrated, for  $^{87}\text{Rb}-^{133}\text{Cs}$  collision, in Table 3 where we have calculated  $a$  and  $\Delta a$  for different values of  $N_e$  and  $n_i$  keeping  $N_e^{in}/N_e^{out} = 6/5$  and  $r_{max} = 6000$  bohr, and employing the same potential as Jamieson *et al* [31].

The Table 3 also demonstrate that, for the energy  $E = 10^{-10}$  hartree, the scattering length calculated with the best base parameters has not yet converged in any decimal place to the same respective values calculated from the lower energies. It means that this energy value does not lead to a good approximation of equation (6). Thus, we consider the energy,  $E$ , of the order of  $10^{-30}$  hartree ensuring a very small  $k$  so that  $a$  is calculated by the equation (6); this energy value is, for example, much lower than the one used by Zanelatto *et al* [33] who considered the energy of the order of  $10^{-13}$  hartree.

Again, employing the same potential as Jamieson *et al* [31], we show in Table 4 the influence of maximum separation,  $r_{max}$ , in the convergence of the scattering length for the  $^{85}\text{Rb}-^{133}\text{Cs}$  and  $^{87}\text{Rb}-^{133}\text{Cs}$  collisions. In the Table 4 we note that

the present results converge to a value very close to those obtained by Jamieson *et al* and Zanelatto *et al* for a large maximum separation; the best agreement is reached in around  $r_{max} = 1000$  bohr, but continues its convergence as the maximum separation increases. Thereby, we evidence the efficiency of the present method to calculate the scattering length.

Now we consider the PEC, proposed by Almeida *et al* [25], with spectroscopic accuracy, obtained for  $X^1\Sigma^+$  state of RbCs, from a direct adjustment procedure of experimental data based on the genetic algorithm. It is given by equation (13) and Table 1. In Table 5 we show the scattering length for  $^{85}\text{Rb}-^{133}\text{Cs}$  and  $^{87}\text{Rb}-^{133}\text{Cs}$  collisions. The present results were obtained using the FEM with  $N_e = 60$  in the interval  $[0, 40]$  bohr,  $N_e = 50$  in the interval  $[40, 6000]$  bohr and  $n_i = 30$ . Also, in the table, results are shown for various PECs using several sets of short and long range data withdrawn of Refs. [31] and [33]. Note that the scattering length is very sensitive to the PEC parameters. The maximum values found in the Table correspond to the set IV calculated by Jamieson *et al* [31] using the iterated perturbation analysis (IPA) potential by Fellows *et al* [34] for the short-range interaction and the long-range data from the equation (14) smoothing to IPA potential. In turn, the minimum values of  $a$  correspond to the set VIII calculated by Zanelatto *et al* [33] using the *ab initio* short-range potential by Allouche *et al* [35], the dispersion coefficients  $C_6$  obtained in reference [36],  $C_8$  and  $C_{10}$  obtained of reference [37], and the exchange parameters ( $A$ ,  $\beta$  and  $\gamma$ ) obtained in reference [35]. The same short-range data and dispersion coefficients of set VIII were used by Jamieson *et al* [31] using the set VI, but with different exchange parameters. Zanelatto *et al* [33] also used the Fermi function to connect smoothly the terms of short and long range. It is notable that their results are the only ones that have a negative value, indicating a repulsive interaction between atoms.

We also determined the scattering length, for the PEC from Almeida *et al*, using the effective range expansion (7), describing  $k \cot \delta_0$  as a function of  $k^2$ . This is shown in Figure 2 for  $^{87}\text{Rb}-^{133}\text{Cs}$  collision. In order to maintain the results in concordance with the ones obtained by equation (6) we chosen a energy interval between  $10^{-30}$  and  $10^{-20}$  hartree. Then we have got a good estimative for the effective range obtaining  $r_c = 600.903$  bohr for  $^{85}\text{Rb}-^{133}\text{Cs}$  and  $r_c = 473.350$  bohr for  $^{87}\text{Rb}-^{133}\text{Cs}$ .

In particular, the results obtained with the PEC obtained with spectroscopic quality employing the FEM is closer of set VII, also calculated by Jamieson *et al* using their *ab initio* short-range interaction potential and the theoretical values of the long-range parameters obtained in references [37,38] but with  $C_6$  replaced by very precise value of Derevianko *et al* [36]. On the other hand, Almeida *et al* [25] determine the coefficients of multipolar electrostatic expansion of the interaction between the two atoms of the diatomic molecules comparing them with other values reported in the literature. They demonstrated that their results are those with the best agreement considering an experimental estimation of  $\chi_4 = C_6 C_{10} / C_8^2$  close to  $4/3$ , as suggested by Le Roy [39] based on the observation of the coefficients for electronic states of  $\Sigma$  symmetry. Also the analysis of Thakkar [40] and Mulder *et al* [41] suggests a value of  $\chi_4$  larger than 1.2. This

can be seen in Table 6 in which are presented the coefficients of multipolar electrostatic expansion taken from Table 1 and from several sets of Table 5. Thus, the  $C_6$ ,  $C_8$  and  $C_{10}$  values of Almeida *et al* indicate good estimate for the dispersion coefficients. This lead us to consider that the results obtained in the present study using the Almeida *et al* PEC represent good estimates for scattering length and effective range of RbCs collision in ground state.

#### 4. Conclusion

In this paper we utilized a numerical procedure based on variational  $R$ -matrix and finite element methods to solve the radial Schrödinger equation and perform the calculation of scattering length for the cold collision between the rubidium and cesium atoms. Also we test a potential energy curve recently fitted to spectroscopic data by Almeida *et al* [25] using a methodology based on genetic algorithm. We notice that our results agree with the previously published in literature. Whereas both variational principle and local basis functions are quite accurate methods for numerical solution of physical problems, we believe that the values displayed here, with the novel potential curve, can be a good estimation for scattering length and effective range of the ground electronic state of RbCs.

We pointed out that we utilize an efficient algorithm for obtaining the  $R$ -matrix based on a matrix inversion technique which has been successfully applied in other studies [23, 24]. This algorithm works with small block matrices and aims to achieve just the last block of the inverse matrix. As the generated matrices by our methodology is very sparse it is needed to keep into the computer's memory just few non-zero blocks. The advantage is that it reduces significantly both memory and computational effort required to invert the matrix, which is generally quite large in variational approaches.

#### Acknowledgments

This work was supported by the Brazilian agencies CNPq, CAPES and FAPESB.

#### References

- [1] J. Weiner. *Cold and Ultracold Collisions in Quantum Microscopic and Mesoscopic Systems*. Cambridge University Press, Cambridge, 2003.
- [2] T. Shimasaki, M. Bellos, C. D. Bruzewicz, Z. Lasner, and D. DeMille. Production of rovibronic-ground-state rbc molecules via two-photon-cascade decay. *Phys. Rev. A*, 91:021401(R), 2015.
- [3] P. K. Molony, P. D. Gregory, Z. Ji, B. Lu, M. P. Köppinger, C. R. Le Sueur, C. L. Blackley, J. M. Hutson, and S. L. Cornish. Creation of ultracold  $^{87}\text{Rb}^{133}\text{Cs}$  molecules in the rovibrational ground state. *Phys. Rev. Lett.*, 113:255301, 2014.
- [4] T. Takekoshi, L. Reichsöllner, A. Schindewolf, J. M. Hutson, C. R. Le Sueur, O. Dulieu, F. Ferlaino, R. Grimm, and H-C Nägerl. Ultracold dense samples of dipolar rbc molecules in the rovibrational and hyperfine ground state. *Phys. Rev. Lett.*, 113:205301, 2014.
- [5] C. D. Bruzewicz, M. Gustavsson, T. Shimasaki, and D. DeMille. Continuous formation of vibronic ground state rbc molecules via photoassociation. *New J. Phys.*, 16:023018, 2014.



- [6] V. Zuters, O. Docenko, M. Tamanis, R. Ferber, V. V. Meshkov, E. A. Pazyuk, and A. V. Stolyarov. Spectroscopic studies of the  $(4)^1\sigma^+$  state of rbc $s$  and modmodel of the optical cycle for ultracold  $x^1\sigma^+$  ( $\nu = 0, j = 0$ ) molecule production. *Phys. Rev. A*, 87:022504, 2013.
- [7] T. Takekoshi, M. Debatin, R. Rameshan, F. Ferlaino, R. Grimm, H-C Nägerl, C. R. Le Sueur, J. M. Hutson, P. S. Julienne, S. Kotochigova, and E. Tiemann. Towards the production of ultracold ground-state rbc $s$  molecules: Feshbach resonance, weakly bound states, and the coupled-channel model. *Phys. Rev. A*, 85:032506, 2012.
- [8] Y. Yang, X. Liu, Y. Zhao, L. Xiao, and S. Jia. Rovibrational dynamics of rbc $s$  on its lowest  $1,3\sigma^+$  potential curves calculated by couple cluster method with all-electron basis set. *J. Phys. Chem.*, 116:11101, 2012.
- [9] O. Docenko, M. Tamanis, R. Ferber, H Knöckel, and E. Tiemann. Singlet and triplet potentials of ground-state atom pair rb+cs studied by fourier-transform spectroscopy. *Phys. Rev. A*, 2011:052519, 2011.
- [10] S. K. Adhikari. *Variational Principles and the Numerical Solution of Scattering Problems*. John Wiley & Sons, New York, 1998.
- [11] E. P. Wigner and L. Eisenbud. Higher angular momenta and long range interaction in resonance reactions. *Phys. Rev.*, 72:29, 1947.
- [12] P. B. Burke. *R-Matrix Theory of Atomic Collisions: Application to Atomic, Molecular and Optical Processes*. Springer-Verlag, Berlin, 2011.
- [13] L. R. Ram-Moham. *Finite Element and Boundary Element Applications in Quantum Mechanics*. Oxford University Press, New York, 2002.
- [14] J. E. Pask, B. M. Klein, P. A. Sterne, and C. Y. Fong. Finite-element methods in electronic-structure theory. *Comput. Phys. Commun.*, 135:1, 2001.
- [15] J. J. Soares Neto and F. V. Prudente. A novel finite element method implementation for calculating bound states of triatomic systems: Application to the water molecule. *Theor. Chim. Acta*, 89:415, 1994.
- [16] F. V. Prudente and J. J. Soares Neto. Optimized mesh for the finite-element method using a quantum-mechanical procedure. *Chem. Phys. Lett.*, 302:43, 1999.
- [17] J. Linderberg, S. B. Padkjær, Y. Öhrn, and B. Vessal. Numerical implementation of reactive scattering theory. *J. Chem. Phys.*, 90:6254, 1989.
- [18] R. Jaquet and U. Schnupf. The  $s$ -matrix version of the hulthén-kohn variational principle for quantum scattering: Comparison between conventional and finite element basis sets. *Chem. Phys.*, 165:287, 1992.
- [19] H. A. Bethe. Theory of the effective range in nuclear scattering. *Phys. Rev.*, 76:38, 1949.
- [20] J. M. Blatt. On the neutron-proton force. *Phys. Rev.*, 74:92, 1948.
- [21] J. M. Blatt and J. D. Jackson. On the interpretation of neutron-proton scattering data by schwinger variational method. *Phys. Rev.*, 76:18, 1949.
- [22] M. N. Guimarães and F. V. Prudente. A study of the confined hydrogen atom using the finite element method. *J. Phys. B: At. Mol. Opt. Phys.*, 38:2811, 2005.
- [23] F. V. Prudente and J. J. Soares Neto. Quantum scattering using a novel implementation based on the variational  $r$  matrix formalism and the finite element method: A comparative study. *Chem. Phys. Lett.*, 309:471, 1999.
- [24] M. N. Guimarães and F. V. Prudente. A variational adiabatic hyperspherical finite element  $r$  matrix methodology: General formalism and application to h+h $_2$  reaction. *Eur. Phys. J. D.*, 64:287, 2011.
- [25] M. M. Almeida, F. V. Prudente, C. E. Fellows, J. M. C. Marques, and F. B. Pereira. Direct fit of spectroscopic data of diatomic molecules by using genetic algorithms: Ii. the ground state of rbc $s$ . *J. Phys. B: At. Mol. Opt. Phys.*, 44:225102, 2011.
- [26] K. T. Tang and J. P. Toennies. An improved simple model for the van der waals potential based on universal damping functions for dispersion coefficients. *J. Chem. Phys.*, 80:3726, 1984.
- [27] T. Korona, H. L. Williams, R. Bukowski, B. Jeziorski, and K. Szalewicz. Helium dimer potential

- from symmetry-adapted perturbation theory calculations using large gaussian geminal and orbital basis sets. *J. Chem. Phys.*, 106:5109, 1997.
- [28] K. Patkowski, G. Murdachaew, C.-M. Fou, and K. Szalewicz. Accurate *ab initio* potential for argon dimer including highly repulsive region. *Mol. Phys.*, 103:2031, 2005.
  - [29] F. V. Prudente, J. M. C. Marques, and A. M. Maniero. Time-dependent wave packet calculation of lih+h reactive scattering on new potential energy surface. *Chem. Phys. Lett.*, 474:18, 2009.
  - [30] J. M. C. Marques, F. V. Prudente, M. M. Almeida, and C. E. Fellows. A new genetic algorithm to be used in the direct fit of potential energy curves to *ab initio* and spectroscopic data. *J. Phys. B: At. Mol. Opt. Phys.*, 41:085103, 2008.
  - [31] M. J. Jamieson, H. Sarbazi-Azad, H. Ouerdane, G.-H. Jeung, Y. S. Lee, and W. C. Lee. Elastic scattering of cold caesium and rubidium atoms. *J. Phys. B: At. Mol. Opt. Phys.*, 36:1085, 2003.
  - [32] W. H Press, S. A Teukolsky, W. T. Vetterling, and B. P. Flannery. *Numerical Recipes in Fortran 77: The Art of Scientific Computing*. Cambridge University Press, New York, 2 edition, 1992.
  - [33] A. L. M. Zanelatto, E. M. S. Ribeiro, and R. d. J. Napolitano. Scattering lengths for li-cs, na-cs, k-cs and rb-cs ultracold collisions. *J. Chem. Phys.*, 123:014311, 2005.
  - [34] C. E. Fellows, R. F. Gutterres, A. P. C. Campos, J. Vergès, and C. Amiot. The rbc  $x^1\sigma^+$  ground state: New spectroscopic study. *Rep. Prog. Phys.*, 46:97, 1983.
  - [35] A. R. Allouche, M. Korek, K. Fakherdding, A. Chaalang, M. Dagher, F. Taher, and M. Aubert-Frécon. Theoretical electronic structure of rbc revisited. *J. Phys. B: At. Mol. Opt. Phys.*, 33:2307, 2000.
  - [36] A. Derevianko, J. F. Babb, and A. Dalgarno. High-precision calculations of van der waals coefficients for heteronuclear alkali-metal dimers. *Phys. Rev. A*, 63:052704, 2001.
  - [37] M. Marinescu and Sadeghpour. H. R. Long-range potentials for two-species alkali-metal atoms. *Phys. Rev. A*, 59:390, 1999.
  - [38] M. Marinescu and A. Dalgarno. Analytical interaction potentials of the long range alkali-metal dimers. *Z. Phys. D: At., Mol. Clusters*, 36:239, 1996.
  - [39] R. J. Le Roy. Long-range potential coefficients from rkr turning points:  $c_6$  and  $c_8$  for  $b(^3\pi_{ou}^+)$ -state  $cl_2$ ,  $br_2$ , and  $i_2$ . *Can. J. Phys.*, 52:246, 1974.
  - [40] A. J. Thakkar. Higher dispersion coefficients: Accurate values for hydrogen atoms and simple estimates for other systems. *J. Chem. Phys.*, 89:2092, 1988.
  - [41] F. Mulder, G. F. Thomas, and W. J. Meath. A critical study of some methods for evaluating the  $c_6$ ,  $c_8$  and  $c_{10}$  isotropic dispersion energy coefficients using the first row hydrides, co,  $co_2$  and  $n_2o$  as models. *Mol. Phys.*, 41:249, 1980.

**Table 1.** Parameters obtained by the genetic algorithm procedure of direct adjustment. The parameters  $a_i$  are in atomic units.

$a_1$	-1.9504268
$a_2$	0.395953461 <sup>a</sup>
$a_3$	8.2933763
$a_4$	-0.02599482
$a_5$	-0.00030692
$a_6$	0.11351898
$a_7$	0.03321360
$a_8$	0.87509116
$C_6$ ( $\times 10^6 \text{cm}^{-1} \text{\AA}^6$ )	29.783746
$C_8$ ( $\times 10^8 \text{cm}^{-1} \text{\AA}^8$ )	11.085596
$C_{10}$ ( $\times 10^{10} \text{cm}^{-1} \text{\AA}^{10}$ )	4.8508464

<sup>a</sup> It is misspelled in reference [25].**Table 2.** Parameters (in atomic units) used by Jamieson *et al* [31] for obtaining the analytical form of long-range potential.

$C_6$ ( $\times 10^3$ )	5.663
$C_8$ ( $\times 10^5$ )	7.3052
$C_{10}$ ( $\times 10^7$ )	10.831
$A$ ( $\times 10^{-3}$ )	1.5069
$\beta$	5.5060
$\gamma$	1.0797

**Table 3.** Scattering length,  $a$ , and, in parentheses, the convergence factor,  $\Delta a(N_e, n_i) = |a(N_e, n_i) - a(N_e, n_i - 1)|$ , results as function of basis definition ( $N_e$  and  $n_i$ ) being  $N_e = N_e^{in} + N_e^{out}$  with  $N_e^{in}/N_e^{out} = 6/5$ , and for  $r_{max} = 6000$  bohr. Calculated with the potential from Jamieson's *et al* [31] (Figure 1) for the  $^{87}\text{Rb}-^{133}\text{Cs}$  collision in the  $X^1\Sigma^+$  state. All the magnitudes in atomic units:  $m(^{133}\text{Cs}) = 132.905447$  a.u. and  $m(^{87}\text{Rb}) = 86.9091835$  a.u..

Energy	$N_e$	$a$ and $\Delta a$				
		$n_i = 15$	$n_i = 20$	$n_i = 25$	$n_i = 30$	$n_i = 35$
$10^{-10}$	88	14.738319	123.65673	72.010790	70.561921	70.561575
			( $\approx 10^2$ )	( $\approx 10^1$ )	( $\approx 10^0$ )	( $\approx 10^{-4}$ )
	110	-148.75215	74.153436	70.562123	70.561575	70.561575
			( $\approx 10^2$ )	( $\approx 10^0$ )	( $\approx 10^{-4}$ )	( $< 10^{-6}$ )
	154	74.659203	70.562010	70.561576	70.561575	70.561575
			( $\approx 10^0$ )	( $\approx 10^{-4}$ )	( $< 10^{-6}$ )	( $< 10^{-6}$ )
$10^{-15}$	88	-6.4915552	6381.2704	61.630639	60.118525	60.118163
			( $\approx 10^3$ )	( $\approx 10^3$ )	( $\approx 10^0$ )	( $\approx 10^{-4}$ )
	110	241.81065	63.849319	60.118736	60.118163	60.118163
			( $\approx 10^2$ )	( $\approx 10^0$ )	( $\approx 10^{-4}$ )	( $< 10^{-6}$ )
	154	64.370015	60.118618	60.118163	60.118163	60.118163
			( $\approx 10^0$ )	( $\approx 10^{-4}$ )	( $< 10^{-6}$ )	( $< 10^{-6}$ )
$10^{-20}$	88	-6.4919374	6380.3086	61.630452	60.118336	60.117974
			( $\approx 10^3$ )	( $\approx 10^3$ )	( $\approx 10^0$ )	( $\approx 10^{-4}$ )
	110	241.80990	63.849135	60.117974	60.117974	60.117974
			( $\approx 10^2$ )	( $\approx 10^0$ )	( $< 10^{-6}$ )	( $< 10^{-6}$ )
	154	64.369832	60.118429	60.117975	60.117974	60.117974
			( $\approx 10^0$ )	( $\approx 10^{-4}$ )	( $< 10^{-6}$ )	( $< 10^{-6}$ )
$10^{-30}$	88	-6.4919374	6380.3085	61.630452	60.118336	60.117974
			( $\approx 10^3$ )	( $\approx 10^3$ )	( $\approx 10^0$ )	( $\approx 10^{-4}$ )
	110	241.80989	63.849135	60.118548	60.117974	60.117974
			( $\approx 10^2$ )	( $\approx 10^0$ )	( $\approx 10^{-4}$ )	( $< 10^{-6}$ )
	154	64.369832	60.118429	60.117975	60.117974	60.117974
			( $\approx 10^0$ )	( $\approx 10^{-4}$ )	( $< 10^{-6}$ )	( $< 10^{-6}$ )

**Table 4.** Influence of the maximum separation,  $r_{max}$ , in convergence of the scattering length,  $a$ , both in bohr, for the Rb–Cs collision in the  $X^1\Sigma^+$  state, calculated with the potential from Jamieson’s *et al* [31] (Figure 1). Mass, in atomic units:  $m(^{133}\text{Cs}) = 132.905447$  a.u.;  $m(^{85}\text{Rb}) = 84.9117893$  a.u.;  $m(^{87}\text{Rb}) = 86.9091835$  a.u..

	$^{85}\text{Rb}-^{133}\text{Cs}$	$^{87}\text{Rb}-^{133}\text{Cs}$
$r_{max}$	$a$	$a$
200	67.6489	83.8008
300	50.2289	69.5049
400	44.5831	64.5238
500	42.3731	62.5026
600	41.3493	61.5461
700	40.8135	61.0385
800	40.5067	60.7450
900	40.3188	60.5639
1000	40.1972	60.4461
1200	40.0579	60.3102
1400	39.9862	60.2398
1600	39.9456	60.1997
1800	39.9208	60.1753
2000	39.9050	60.1595
6000	39.8634	60.1180

**Table 5.** Scattering length,  $a$ , for various potential energy curves of  $X^1\Sigma^+$  state using several data sets. Mass, in atomic units:  $m(^{133}\text{Cs}) = 132.905447$ ;  $m(^{85}\text{Rb}) = 84.9117893$ ;  $m(^{87}\text{Rb}) = 86.9091835$ .

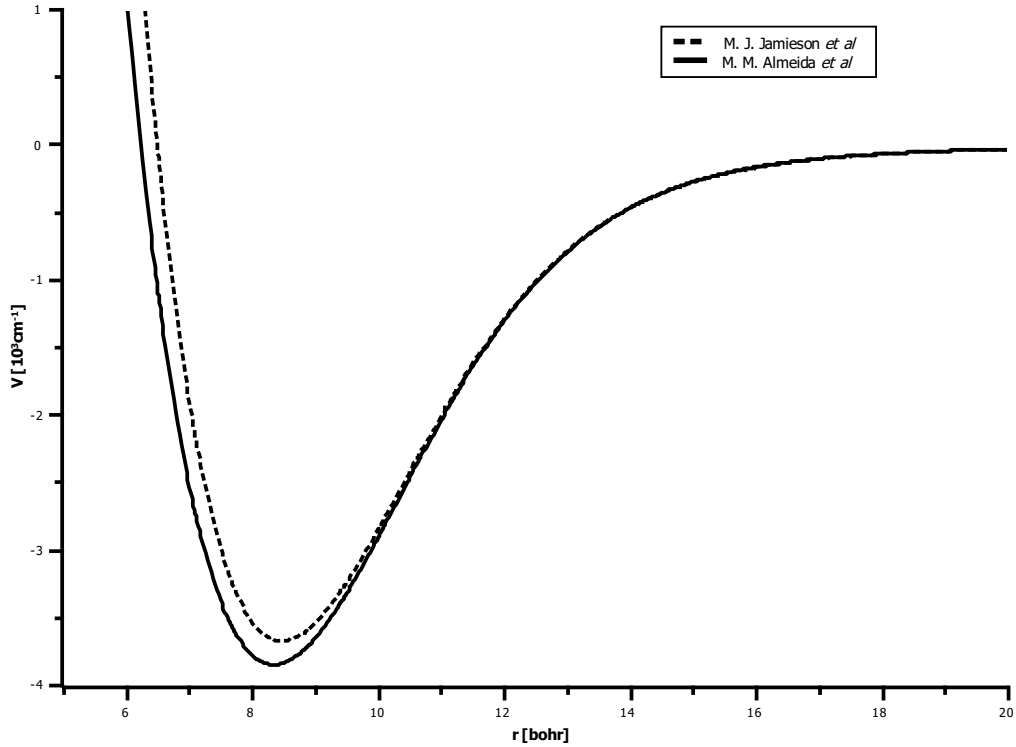
	$^{85}\text{Rb}-^{133}\text{Cs}$	$^{87}\text{Rb}-^{133}\text{Cs}$
Present	59.0770	65.4915
Set I <sup>a</sup>	321.3	417.1
Set II <sup>a</sup>	115.9	126.6
Set III <sup>a</sup>	103.0	112.4
Set IV <sup>a</sup>	380.9	564.2
Set V <sup>a</sup>	27.79	38.87
Set VI <sup>a</sup>	0.0902	12.43
Set VII <sup>a</sup>	40.24	60.18
Set VIII <sup>b</sup>	−40.618	−11.125

<sup>a</sup> Jamieson *et al* [31]

<sup>b</sup> Zanelatto *et al* [33]

**Table 6.** Coefficients of multipolar electrostatic expansion (in atomic units) taken from Table 1 and from several sets of Table 5.

	$C_6$ ( $\times 10^3$ )	$C_8$ ( $\times 10^5$ )	$C_{10}$ ( $\times 10^7$ )	$\chi_4 = C_6 C_{10} / C_8^2$
Almeida <i>et al</i> [25]	6.1800	8.2142	12.836	1.18
Set I	5.2840	7.3052	10.831	1.07
Set II	5.4785	8.566	11	0.82
Set III	5.4798	8.566	11	0.82
Set IV	5.4318	8.581	11	0.81
Set V	5.663	8.566	11	0.85
Set VI–VIII	5.663	7.3052	10.831	1.15

**Figure 1.** Potential energy curve for the  $X^1\Sigma^+$  state of RbCs molecule.

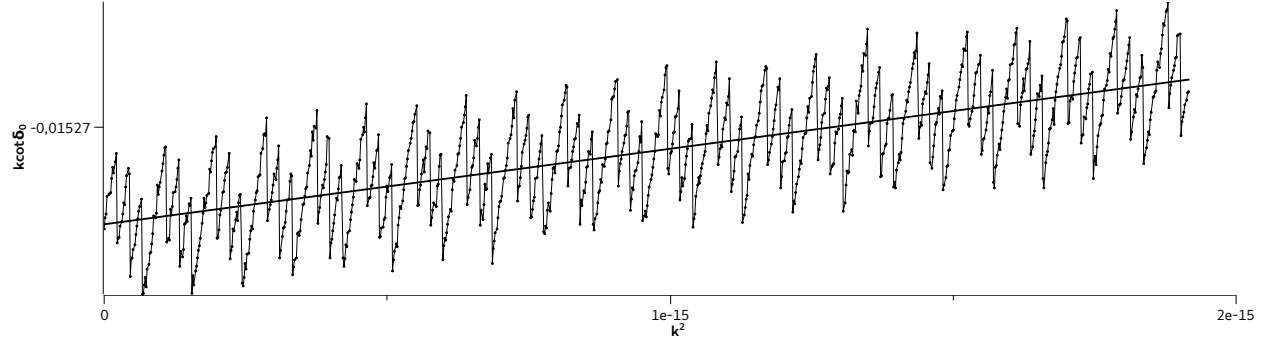


**Figure 2.** Graph of equation (7) describing of  $k \cot \delta_0$  as function of  $k^2$  for  $^{87}\text{Rb}-^{133}\text{Cs}$  collision. The energy  $E = \hbar k^2/2\mu$  varies between  $10^{-30}$  and  $10^{-20}$  hartree. The straight line is the linear regression adjustment getting  $k \cot \delta_0 = -1.5269 \cdot 10^{-2} + 2.3667 \cdot 10^2 k^2$  (a.u.).